sciendo

HRVATSKO FARMACEUTSKO DRUŠTVO
CROATIAN PHARMACEUTICAL SOCIETY

Acta Pharm. **71** (2021) 81–98
https://doi.org/10.2478/acph-2021-0010

Original research paper

Investigation of design space for freeze-drying injectable ibuprofen using response surface methodology

MAJA PRESKAR[1,2,*]
DANIJEL VIDEC[1]
FRANC VREČER[1,2]
MIRJANA GAŠPERLIN[2]

[1] *Krka d.d. SI-8000 Novo mesto, Slovenia*

[2] *University of Ljubljana, Faculty of Pharmacy, SI-1000, Ljubljana, Slovenia*

This study explores the use of a statistical model to build a design space for freeze-drying two formulations with ibuprofen. A 2 × 3 factorial experimental design was used to evaluate independent variables (filling volume and annealing time) and responses as residual moisture content, specific surface area and reconstitution time. A statistical model and response surface plots were generated to define the interactions among the selected variables. The models constructed for both formulations suggest that 1 mL of filled volume and no annealing should be used to achieve optimal residual moisture content, specific surface area and reconstitution time. The proposed models were validated with additional experiments, in which the responses observed were mainly in close agreement with the predicted ones. Additionally, the established models demonstrate the reliability of the evaluation procedure in predicting the selected responses.

Keywords: design space, response surface method, lyophilization, ibuprofen

Accepted April 5, 2020
Published online May 14, 2020

Ibuprofen (IBP) is a weak acid, classified as a Class II (1) drug according to the biopharmaceutical classification system (BCS) (1). It is a member of the well-established nonsteroidal anti-inflammatory drugs (NSAIDs), and it is widely used for acute or chronic pain relief. Due to its poor aqueous solubility (0.12 mg mL^{-1} at 25 °C) (2) and high dosing (the maximum single dose for *per os* application is 800 mg) (3), it presents a great challenge to formulate both solid and liquid dosage forms, including parenteral ones.

Various techniques for increasing the aqueous solubility of IBP in oral solid and liquid formulations described in the literature were briefly reviewed in our previous research (4). Each technique exhibits both advantages and disadvantages, and the choice depends on drug characteristics, pharmaceutical dosage form, and route of application (5), which in our case was freeze-dried powder for parenteral application. Our previous work already demonstrated the development of a freeze-dried product with IBP with the capacity for intravenous (*i.v.*) application by simple reconstitution with a predetermined quantity of

* Correspondence; e-mail: maja.preskar@krka.biz

water for injection (WFI), without any need for additional isotonization (4). Despite the fact that the *i.v.* application shows benefits, a market research study still shows a lack of parenteral products containing IBP, which encouraged us to extended our previous work into this study, that focuses on the optimization of the lyophilization process.

However, lyophilization is an expensive and complex technological process; hence its optimization is at the focus of the pharmaceutical industry (6–8). With the publication of the International Conference on Harmonization (ICH) Q9 guideline on quality risk management, the application of recent development approaches such as quality by design (QbD) and process analytical technology (PAT) with the design of experiments (DoE) is becoming an expectation not only from the regulatory standpoint but also from a quality perspective (6, 9). Risk management tools and the choice among them depend on specific facts and requirements of the formulation. Thus, for the implementation of QbD, an understanding of both the product and the process is necessary (10, 11).

Studying the effects of formulation parameters on critical process parameters and product quality attributes by trial and error or by changing one separate factor at a time (COST) strategies is inefficient, mostly because the data from these experiments do not make it possible to identify interaction effects among the variables. Therefore, a DoE methodology was applied (8). The COST approach also often does not lead to the optimum solution within the space investigated, whereas DoE allows the determination of a design space around the optimum settings within which the desired responses are guaranteed (8).

The objective of this study was to demonstrate how the response surface method (RSM), one of the DoE methods, efficiently optimizes formulation and process variables and identifies the desired combination within the design space for the freeze-dried product with IBP. In addition, the levels of the design parameters at which responses reach optimum were defined.

The increased number of publications with new approaches in QbD for the freeze-drying process emphasizes the fact that the freeze-drying process is suitable for the application of QbD principles (6). However, most studies focus on process optimization of the longest step in the freeze-drying process; namely, primary drying (12, 13).

Thus, gaining an understanding of the influence and interaction of formulation and process parameters of freeze-dried IBP products could open new possibilities for developing an appropriate control strategy. These parameters include filling volume and annealing time on drug product quality responses such as residual moisture content (RMC), specific surface area (SSA), and reconstitution time (RT), and defining the design space by QbD.

EXPERIMENTAL

Materials

Crystalline IBP was provided by Krka d.d, Slovenia. For lyophilized product preparation, an ingredient for pH adjustment (L-arginine, provided by Ajinomoto Omnichen n.v.), isotonic agents (mannitol, provided by Roquette Italy s.p.a. and sodium chloride (NaCl), provided by Salinen Austria AG), and co-solvent (tertiary butyl alcohol, provided by Sigma-Aldrich) were used.

Preparation of freeze-dried powders

Solutions for freeze-drying were prepared according to the requirements for parenteral products with regard to tonicity and pH. Two formulations were prepared with different isotonic agents: sodium chloride (NaCl) and mannitol. Both are commonly used but have very different characteristics (*i.e.*, solubility, crystallization behavior and polymorphism) (4). The quantity of mannitol or NaCl was defined with respect to achieving osmolality criteria in a range of 280–320 mOsmol kg^{-1} of the reconstituted powder, and the quantity of L-arginine by pH criteria (following the optimal physiological pH of 7.4). IBP was dissolved in tertiary butyl alcohol and further mixed with L-arginine and mannitol or NaCl, followed by filtration through a 0.22 μm filter. The concentration of IBP in the solution for freeze-drying was 12 mg mL^{-1}. Afterward, 2 mL of prepared solution was placed in a 10 mL vial and lyophilized. The batch size of each experiment was 100 vials of F1 or F2 solution, surrounded by vials filled with water. A Minifast 10 (IMA Life Pharmaceutical Systems) with four shelves and a capacity of 0.8 m^2 was used to freeze-dry the samples. The freeze-drying cycle was performed at –45 °C for 3 h and then –30 °C and a pressure of 17.7 Pa for 12 h, followed by 5 h at –10 °C and 4 h at 5 °C. Secondary drying was performed at 30 °C for 6 h at 17.7 Pa. Table I shows the compositions of the experimental formulations.

Table I. Composition formula of F1 and F2

	F1	F2
Ibuprofen	12 mg	12 mg
Mannitol	–	150 mg
Sodium chloride	27 mg	–
Tertiary butyl alcohol	156 mg	156 mg
L-arginine	10.4 mg	10 mg
WFI	up to 1 mL	up to 1 mL

Characterization of thermal behavior of lyophilized formulations

In order to define the temperature and pressure conditions for the lyophilization process, the characterization of formulation to be freeze-dried was performed and taken into consideration. This involved in particular the glass transition temperature (T_g') and collapse temperature (T_c) for an amorphous system or eutectic temperature (T_{eu}) for a crystalline system. The methods most often applied for characterization of critical temperatures for materials to be freeze-dried are differential scanning calorimetry (DSC), modulated DSC, and freeze-dried microscopy (FDM).

Differential scanning calorimetry (DSC)

A Mettler Toledo DSC1 was used to study the thermal behavior of IBP and its changes in F1 and F2 samples. Approximately 3 mg samples were weighed in standard aluminum

pans and sealed with a perforated aluminum lid. An empty pan was used as a reference. The samples were first cooled from 20 to –70 °C with a cooling rate of 10 K min^{-1} and an isothermic hold at –70 °C for 30 min, and they were then heated from –70 °C to 40 °C at a heating rate of 10 K min^{-1}. A dynamic nitrogen atmosphere with a flow rate of 40 mL min^{-1} was used during the experiment.

Freeze-drying microscopy (FDM)

The formulations were analyzed by a Lyostat FDM (Linksys 32) equipped with Linkam software for image and data capture. An approximately 2 μL sample of each of the solutions F1 and F2 were treated according to the temperature profile described below (with and without annealing). Each solution was analyzed in duplicate. The results are presented as an average.

For the procedure without annealing, the sample was cooled to –45 °C at a rate of 5 °C min^{-1} and held at this temperature for 10 min before a vacuum of 1 Pa was applied.

For the procedure with annealing, the sample was cooled to –45 °C at a rate of 5 °C min^{-1} and was then ramped to –30 °C at 5 °C min^{-1} and held for 10 min to anneal. The sample was then cooled back to –45 °C at 5 °C min^{-1} for 10 min and afterward, a vacuum of 1 Pa was applied.

Measurement of the reconstitution time (RT)

Each vial with lyophilized powder contained 12, 24, or 36 mg of IBP. In order to prepare the target IBP concentration for parenteral preparation (*i.e.*, 4 mg mL^{-1}), 3, 6, or 9 mL of WFI was added to the finished product (14). Afterward, the vials were manually shaken and the time until a clear solution, determined by the naked eye, was measured.

Measurement of the residual moisture content (RMC)

Measurement of the RMC was performed using the Karl Fischer method (Ph. Eur. 2.5.12) (methanol, anhydrous, *p.a.*). The water content of methanol was determined. The vial with the lyophilizate was weighed and afterward diluted with 3.0 mL of methanol. The vial content was homogenized first by manual shaking, continuing in an ultrasound bath, and finally centrifuged at 4,000 rpm for 10 min. One mL of the sample solution obtained was withdrawn, and the water content was determined using the Karl Fisher method. The RMC was determined on a single vial in duplicate.

The final water content in the IBP lyophilizate was calculated according to Eq. *1*:

$$\%\, of\ residual\ moisture\ content = \frac{100}{100 - c} \times \left(\frac{c \times m_{sol}}{m_{ext}} - \frac{B \times m_{sol}}{m_{ext}} \right) \qquad (1)$$

where C is residual moisture content determined with the Karl Fisher method (%), B is water content of methanol (%), m_{sol} is mass of the added methanol (g) and m_{ext} is the average mass of IBP freeze-dried powder (g). Afterward, RMC was expressed in mg per vial, using the result from Eq. *1* and individual cake mass.

Measurement of specific surface area (SSA)

BET (Brunauer-Emmett-Teller) surface area analyses of materials by nitrogen multilayer adsorption were used (Micromeritics TriStar 3000 analyzer). Before the measurement, the samples were degassed at 60 °C for 1 h until the mass reached a constant value.

Experimental design

In order to optimize the freeze-drying process and the product itself to target specification, experiment results were analyzed and evaluated by Design Expert 10.0 and JMP 13 (SAS Institute Inc., Cary, NC, USA), using a 2 × 3 factorial design of the first variable (filling volume) at high, middle, and low levels and the second variable (annealing time) at low and high levels. To maintain all the advantages of the product, such as osmolality after reconstitution with WFI, formulation variables such as API and excipient concentration, and vial size were eliminated by using the same compositions and standard 10-mL vial.

A linear regression model was constructed and statistical evaluation of the model was performed in the form of analysis of variance (ANOVA). The *p*-value, coefficient of determination (R^2), adjusted coefficient of determination (R^2_{adj}), predicted coefficient of determination (R^2_{pred}), and normalized root-mean-square error (NRMSE) were calculated. Six runs of each formulation were performed.

Afterward, the validation of the predictive model was performed. RMC, SSA, and RT were estimated according to the equations described in the section on validation of the predictive model through new experiments. To obtain the theoretical values of RMC (Z1), SSA (Z2), and RT (Z3), the exact values of the filling volume (X1) and annealing time (X2) were substituted in the equations.

RESULTS AND DISCUSSION

Freeze-drying process development

The development of the freeze-drying process is based on representative and accurate measurements of the critical process temperatures. First, to define T_{eu} or T_g', T_c, and $T_{melting}$,

Table II. Critical temperatures of F1 and F2

		F1	F2
Freezing temperature (°C)	DSC (Tonset)	–28 to –31	–28.5
	FDM	–28	–28
T_g' or T_{eu} (°C)	DSC	–25	–27
T_c without annealing (°C)	FDM	–29	–26
T_c with annealing (°C)		–30	–34
$T_{melting}$ (°C)	FDM	–15	–12

DSC – differential scanning calorimetry, FDM – freeze-dried microscopy, T_c – collapse temperature, T_{eu} – eutectic temperature, T_g' – glass transition temperature, T_m – melting temperature

the prepared solution was characterized by DSC and FDM. The results are presented in Table II.

The freezing step is a complex process and has been identified as a particularly important phase, which must be well defined, monitored, and controlled because it impacts both the primary and secondary drying and therefore the quality of the finished product (15). The freezing point was characterized by both – DSC and FDM. The freezing temperature of the F1 solution detected by DSC was between –28 and –31 °C, whereas measured by FDM it was –28 °C. The freezing temperature values of the F2 solution detected by DSC and FDM were practically the same (–28.5 °C *vs.* –28 °C). However, in order to ensure complete solidification of different filling volumes of solution (1–3 mL), the worst-case freezing temperature was chosen (the minimum temperature of shelves); namely, –45 °C.

T_{eu} for crystalline material and T_g' for amorphous material together with T_c define the maximum allowable value of product temperature (T_p) during primary drying. T_g' or T_{eu} determined by DSC was –25 °C for F1, whereas for F2 it was –27 °C because T_c was determined by FDM and was higher for F2, but lower for F1. When T_p exceeds T_c which is normally a few degrees above T_g' (16), collapse may occur, and collapse may also occur when T_p exceeds T_g' and results in viscous flow and loss of the established microstructure. Based on these results, T_g' (–25 °C) and T_c (–29 °C) of F1 are in disagreement with the literature data, which states that T_c is usually about 2 °C higher than T_g' (17). Because DSC analyses are performed under more static conditions and represent a more conservative limiting temperature (18) and FDM is based on a subjective evaluation of the onset collapse (19), the shelf temperature (T_s) for primary drying was set at –30 °C. Because T_p was lower than T_c, structure loss behavior was avoided (18, 20).

According to the results presented in Table II, it is evident that, despite different compositions, the measured temperatures of F1 and F2 differed only slightly, and therefore the process parameters presented in Table III were set the same for both formulations.

Lyophilization involves three complex process phases; namely, freezing, primary drying, and secondary drying. They are highly correlated. A typical hold step determined as the annealing phase was performed above T_g' for complete crystallization of bulking

Table III. Process parameters of freeze-drying cycle for F1 and F2

	Temp (°C)	Ramp (min)	Hold (min)	Pressure (Pa)
Loading	10			
Freezing	–45	55	180	
Annealing[a]	–21	96	180	
Freezing	–45	24	180	
Primary drying	–30	60	720	17.7
Primary drying	–10	60	300	17.7
Primary drying	5	120	240	17.7
Secondary drying	30	120	360	17.7

[a] Annealing was alternatively implemented.

agents (19) and was implemented as the variable process factor in the freeze-drying cycle. After ice nuclei were formed and the formulation was completely frozen, the shelf temperature was raised several degrees above T_g', but still below the temperature of ice melting, which is in agreement with literature data (21, 22). The temperature chosen for the annealing process was –21 °C, which is still above T_g' and at the same time below the melting temperature (–15 °C and –12 °C) of both formulations. The temperature of annealing was held for 3 hours and then cooled back to the initial freezing temperature.

Design of the experiment

Critical formulation and process parameters. – For this study, the main question was whether it is possible to estimate the effect of main independent variables and build quality into the freeze-drying process by relying on previous studies and by using DoE. The first step was the identification of the formulation and process parameters affecting the quality of the freeze-drying process and final quality attributes. An extensive list of variables, generally critical for a freeze-drying process was already given in a published review (8). Because it was not feasible to include all of these variables in a risk assessment, selection of the parameters was performed based on previous investigations (16, 23).

Filling volume was already described as a variable that can influence the duration of ice nucleation and, consequently, the freezing and primary drying process (8). Arshad *et al.* (23) also studied freezing characteristics at different fill factors and observed an influence of fill height on the onset of freezing time and consequently altered heat flow during primary drying (23). However, the influence of filling volume on quality attributes of finished products such as RMC, SSA, and RT, was not yet evaluated.

The second independent variable was chosen among the processing parameters. Thermal treatment or annealing, which has a great influence on the size and dispersion of ice crystals, was applied and evaluated.

The rationale for annealing is based on glass transition-associated mobility, which increases dramatically above T_g' and can influence the final product's solid-state (8). Annealing not only reduces heterogeneity in the drying rate caused by variation in ice nucleation but can also result in an increased primary drying rate by as much as a factor of 3.5 due to increased pore diameters (15, 22, 24). The annealing process can also prevent the formation of a skin layer on the top of the cake, thus increasing the sublimation rate (15) and consequently higher porosity and lower residual moisture. On the other hand, previous studies have shown that the annealing step, due to the formation of pore geometries, suppressed the sublimation and desorption rates (23, 25), resulting in the product's reduced SSA, which may lead to higher RMC or require longer secondary drying (22, 26).

Based on contradictory data in the literature, the effects of the annealing process on responses (namely, the quality attributes of the finished product) were evaluated.

Experimental design analyses and evaluations. – In order to optimize the freeze-drying process and the product itself to the target specification, experimental results were analyzed and evaluated with RSM, using a 2 × 3 factorial design. Six experiments were conducted for each formulation (F1 and F2).

The filling volume of the prepared solution (X1) at levels of 1, 2, or 3 mL and the annealing process time (X2) at levels of 0 or 180 min were selected as independent variables.

Table IV. Independent variables, their levels and responses of the factorial design

	Run	Independent variables		Responses		
		Filling volume (mL) (X1)	Annealing time (min) (X2)	Residual moisture content (mg) per vial (Z1)	Specific surface area ($m^2\ g^{-1}$) (Z2)	Reconstitution time (s) (Z3)
F1	1	1	0	0.51	16.3	2
	2	2	0	1.05	14.7	19
	3	3	0	1.16	13.0	22
	4	1	180	0.65	5.8	7
	5	2	180	1.02	7.1	20
	6	3	180	1.31	6.2	25
F2	1	1	0	1.19	16.8	5
	2	2	0	1.89	8.4	6
	3	3	0	3.1	6.8	11
	4	1	180	1.19	8.8	9
	5	2	180	1.62	7.3	10
	6	3	180	2.42	3.3	15

RMC (Z1), SSA (Z2), and RT (Z3), singled out by many studies as critical characteristics (13, 15, 16, 23), were used as responses (Table IV).

Although the acceptance criterion of responses was not defined, it is obvious that lower RMC, higher SSA, and lower RT are desired, which is in agreement with the literature data (16). In addition, the objective for RMC would be below 2 % (*m*/*m*), and preferably less than 1 % (*m*/*m*) (26, 28).

Different filling volumes (1, 2, or 3 mL) were chosen due to the IBP doses needed for the application (14), whereas the levels for annealing time were defined according to suggested times in the literature (23, 26, 29). With regard to process efficiency, the aim of this study was also to determine the shortest freeze-drying process possible, which was evaluated through a comparison between product temperature and shelf temperature, a Pirani gauge sensor-Capacitance manometer (CM) differential and the temperature of the condenser. However, the product quality characteristics above were prioritized.

Freshly prepared lyophilized powders were subjected to further characterization. Combinations of variables and the results of responses are presented in Table IV.

Furthermore, because this study sought to investigate the effects of independent variables and their optimization, a linear regression model was constructed and statistical evaluation of the model was performed using ANOVA. The results showed that the models used to fit the responses variables were significant ($p < 0.05$) and adequate to represent the relationship between the response and the independent variables. Additionally, model fitting was evaluated with R^2_{adj} and NRMSE followed by cross-validation using R^2_{pred}. The results are presented in Table V.

Table V. ANOVA statistical testing of linear regression model, for F1 and F2 (training set)

		F1 main effects and comment			F2 main effects and comment		
		Filling volume (X1)	Annealing time (X2)	Linear model	Filling volume (X1)	Annealing time (X2)	Linear model
Residual moisture content (Z1)	*p*-value	0.0095	1	Only the main effect of X1 was identified as active. However, the main effect of X2 was also included in the model because the effect of X2 on the response was our research question. The *p*-value of the model is below 0.05, at 0.022.	0.0009	0.0982	Without transformation, the *p*-value is 0.0166, whereas with inverse square root transformation the value is much lower, 0.0019. In addition, the Box- Cox lambda value (–0.5) also indicates a need for transformation. Furthermore, transformation can be justified with more normal distribution of residuals.
	R^2	0.9216			0.9845		
	R^2_{adj}	0.8693		Adjusted and predicted R^2 are not in reasonable agreement (the difference is more than 0.2).	0.9742		Adjusted and predicted R^2 are in reasonable agreement (the difference is less than 0.2.). If transformation were not implemented, the difference would be more than 0.2.
	R^2_{pred}	0.6261			0.9146		
	NRMSE	11.65			3.01		
Specific surface area (Z2)	*p*-value	0.3263	0.0031	Only the main effect of X2 was identified as active. However, the main effect of X1 was also included in the model because the effect of X1 on the response was our research question and the model would otherwise be underfitted. The *p*-value of the model is below 0.05, at 0.0071.	0.0176	0.0526	A model with only a main effect with square root transformation is used. Furthermore, transformation can be justified with more normal distribution of residuals. Although the influence of X2 is at the limit of significance, both parameters were evaluated, because otherwise the model would be underfitted.
	R^2	0.9631			0.9151		
	R^2_{adj}	0.9384		Adjusted and predicted R^2 are in reasonable agreement (the difference is less than 0.2).	0.8585		Adjusted and predicted R^2 are in reasonable agreement (the difference is less than 0.2).
	R^2_{pred}	0.8124			0.6846		
	NRMSE	12.14			9.74		

Reconstitution time (Z3)	*p*-value	0.0159	0.4097	Only the main effect of X1 was identified as active. However, the main effect of X2 was also included in the model because the effect of X2 on the response was our research question. The *p*-value of model is below 0.05, at 0.0344.	0.0187	0.0288	A model with square root transformation is used, which can be justified with more normal distribution of residuals. The *p*-value of the model is 0.0203.
	R^2	0.8942			0.9256		
	R^2_{adj}	0.8236		Adjusted and predicted R^2 are in reasonable agreement (the difference is less than 0.2).	0.8759		Adjusted and predicted R^2 are in reasonable agreement (the difference is less than 0.2).
	R^2_{pred}	0.6324			0.7312		
	NRMSE	24.29			6.97		

NRMSE – normalized root-mean-square error, R^2 – coefficient of determination, R^2_{adj} – adjusted coefficient of variation, R^2_{pred} – predicted coefficient of determination

Table VI. Comparison of model predictions to experimental results of testing set

	Independent variables		Responses								
	Filling volume (mL) (X1)	Annealing time (min) (X2)	Residual moisture content per vial (mg) (Z1)			Specific surface area (m^2 g^{-1}) (Z2)			Reconstitution time (s) (Z3)		
			Predicted	Experimental	NRMSE	Predicted	Experimental	NRMSE	Predicted	Experimental	NRMSE
F1	1	90	0.62	0.57	32.09	11.09	8.8	17.12	6.33	7	9.80
	2	120	0.94	0.95		8.86	8.4		16.33	16	
	1.5	0	0.78	1.3		15.21	17.2		9.58	7	
	R^2_{pred}[a]				0.6261			0.8124			0.6324
F2	1	90	1.19	1.34	18.22	12.31	17	31.80	6.34	10	47.53
	2	120	1.70	1.85		7.46	16.8		9.73	30	
	1.5	0	1.50	0.91		12.47	9.4		5.87	8	
	R^2_{pred}[a]				0.9146			0.6846			0.7208

[a] Values of the training set, already presented in Table V. NRMSE – normalized root-mean-square error, R^2_{pred} – predicted coefficient of determination

Despite the fact that a limited number of experiments were performed, models for both of the formulations, presented in Table V, can be used to navigate the design space for RMC, SSA, and RT. All the models were constructed including both main effects, indicating that there are no active secondorder effects (interaction or square effects). Additionally, when the transformation of the model can be justified (9), it has been used (Table V).

The regression model of RMC showed the value of R^2 for F1 is 0.9216, which means that the calculated model was able to explain 92.16 % of the total variation in the results, whereas for F2 it is 0.9845. The results indicate that the models used to fit the response variable were significant for both formulations, with p = 0.022 for F1 and 0.0019 for F2, showing adequacy for presenting the relationship between the response and the independent variables. Despite the fact that the annealing time (X2) has no effect on the RMC (p = 1) for F1 and no significant effect (p = 0.0982) for F2, its evaluation was still included in statistical testing because the main goal of this study was the evaluation of both variables. Furthermore, with the inclusion of the X2 effect, the models for both formulations were still significant. According to literature data, R^2 should be expressed in a more advanced version, presented as R^2_{adj} (30, 31), which compares the explanatory power of regression models that contain different numbers of predictors. R^2_{adj} is 0.8693 for F1, indicating that 13.07 % of the total variations are not explained by the model, whereas for F2 the percentage is much lower; that is, 2.58 % (R^2_{adj} = 0.9742). The complementary coefficient is R^2_{pred}, which is 0.6261 for F1 and 0.9146 for F2, and it indicates how well a regression model predicts responses for new observations. R^2_{adj} and R^2_{pred} are always lower than R^2, and their key benefit is that they do not increase in an overfitting condition, in contrast to an incorrectly high value of R^2, which leads to a decreased ability to predict (30, 31). An additional parameter for evaluation of the model, considered as a percentage error, NRMSE, was calculated. Whereas the rootmeansquare error (RMSE) measures the standard deviation of the residuals and is expressed in the same units of measure as the response variables, NRMSE is its coefficient of variation, expressed as a percentage. The NRMSE of F1 for RMC is 11.65, whereas for F2 it is 3.01 and it correlates with R^2_{adj}, indicating high precision and no systematic errors. Based on the evaluation of the training set, it can be concluded that the F2 model for RMC fits the data better than F1; however, both of the models show reasonably good fit.

The chosen model for SSA of F1 yielded R^2 of 0.9631, whereas for F2, where square root transformation was implemented, it was 0.9151. The significance of the model was evaluated with a p-value, which is lower than 0.05 for both formulations (Table V). Due to the evaluation of the main effects of both variables on the chosen responses, X1 and X2 were included, despite the fact that the filling volume's effect is not significant in F1, nor is the time of annealing in F2. A comparison of NRMSE and R^2_{adj} of F1 and F2 shows that the parameters do not correlate, which is additionally explained in the following validation of the predictive models through additional experiments.

When evaluating the fit of the training set, both models fit the data relatively well. However, the model for formulation F1 has higher R^2_{pred}, which indicates less overfitting.

RT was evaluated by a linear model for F1 and square root transformation for F2. Both models are significant and can be used for further studies (p = 0.0344 for F1 and 0.0203 for F2). However, the effect of annealing time in F1 is not significant. In order to evaluate both variables, the main effect of X2 was included. Evaluation parameters indicate

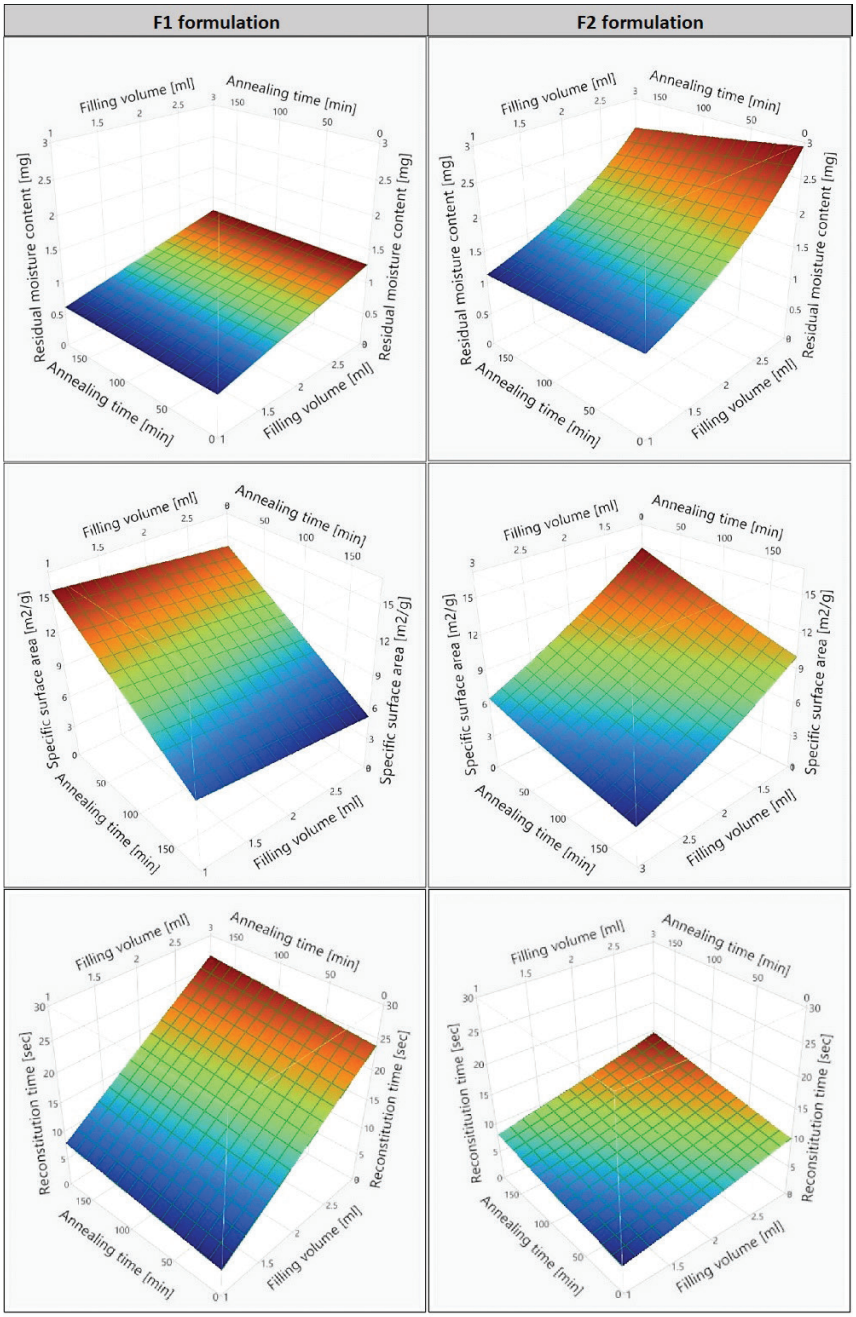

Fig. 1. 3D response surfaces for RMC, SSA, and RT of F1 and F2 formulation. RMC – residual moisture content, RT – reconstitution time, SSA – specific surface area.

a better fit of the model for formulation F2 because R^2_{adj} is higher and NRMSE is lower, indicating that the model for F2 has a lower deviation of residuals.

Finally, ANOVA results show that filling volume has a greater effect than annealing time on all three responses in both formulations, except on SSA of F1. The reason could be in analytical error, vial-to-vial variation, a limited number of trials or the composition formula, because NaCl, which is present in F1, is not a bulking agent, meaning that the effect of filling volume on SSA could be minimized. Contrary to the effect of filling volume, increased annealing time slightly increased RMC, but decreased SSA and RT, which could be explained by increased resistance of the dried layer and primary drying time (27). Even though the effect of annealing time proved to be significant ($p < 0.05$) for only one response in each formulation, the *p*-values are generally lower for formulation F2, showing that, like filling volume, annealing time has a greater influence on responses in formulation F2.

Moreover, our results show a good correlation between responses because samples with lower RMC have higher SSA and consequently shorter RT, which is in good agreement with literature data (16).

The relationship between independent and dependent variables was also graphically presented by the 3D response surface (13) generated by the model, shown in Fig. 1.

Fig. 1 shows the influence of filling volume (X1) and annealing time (X2) on RMC (Z1), SSA (Z2), and RT (Z3) of F1 and F2. For formulations F1 and F2, increasing the filling volume from 1 to 3 mL increases RMC and RT, whereas the effect decreases on SSA for F2 and is not significant for F1 ($p > 0.05$). On the other hand, increasing the annealing time from 0 to 180 min for formulation F1 significantly influences only the SSA, which decreases, whereas the effect on RT and on RMC is not significant. The 3D response surface for F2 shows that increasing the annealing time from 0 to 180 min significantly influences only RT, which increases, whereas the effect on SSA is limited ($p \approx 0.05$) and on RMC it is not significant ($p > 0.05$).

It was shown that the highest SSA and the lowest RT were achieved when using 1 mL of filling volume and no annealing process. However, the lowest RMC is at 1 mL filling volume, with or without the annealing process, because there is no significant effect of X2 on Z1 ($p > 0.05$).

The aim of this study was confirmed. The conditions that yielded minimum RMC, minimum RT, and maximum SSA were determined. Moreover, the goal with the direction of variables, which represents the closeness of a response to its ideal value, called desirability, was defined. The more closely the response approaches the ideal intervals or ideal values, the closer to 1 the desirability is (32). The software generated desirability for both formulations, which was above 0.89, with the optimum filling volume of 1 mL and time of annealing 0 min. Interestingly, influences are similar in both formulations, despite different compositions. The optimal combination is also supported by the duration of primary drying, which was not drastically affected by any of the variables studied.

Validation of the predictive model through new experiments. – To confirm the selected models, their prediction was validated using three additional experimental runs by varying the two independent variables within the first set levels. RMC, SSA, and RT were estimated in accordance with Eqs. *2*, *3*, and *4* for F1 and with Eqs. *5*, *6*, and *7* for F2.

F1

$$Z1 = 0.28833 + 0.32750 \times X1 - 1.07017 \times 10^{-18} \times X2 \quad (2)$$

$$Z2 = 16.31667 - 0.73500 \times X1 - 0.049926 \times X2 \quad (3)$$

$$Z3 = -4.6667 + 9.50000 \times X1 + 0.016667 \times X2 \quad (4)$$

F2

$$\frac{1}{\sqrt{Z1}} = 1.04866 - 0.15565 \times X1 + 2.46562 \times 10^{-4} \times X2 \quad (5)$$

$$\sqrt{Z2} = 4.52207 - 0.66025 \times X1 - 3.92558 \times 10^{-3} \times X2 \quad (6)$$

$$\sqrt{Z3} = 1.69062 + 0.48839 \times X1 + 3.76496 \times 10^{-3} \times X2 \quad (7)$$

A comparison of the predicted values and actual values in Table VI shows that the models constructed are mainly able to predict the response in question with relative accuracy, especially considering factors affecting the process and experimental errors (vial-to-vial variation, outliers, and analytical error) (33). However, some outliers within additional experiments are still present in some models, which is expected because the model was constructed with limited data points.

Based on the results presented in Tables V and VI, it follows that models for RMC are acceptable for both the F1 and F2 formulations. Furthermore, the value of NRMSE for the testing and training set and graphs of actual *versus* predicted values presented in Fig. 2 confirm higher R^2_{adj} for F2 in the training set and show that the model for F2 has a better fit. Additionally, R^2_{pred} of the training set is in good agreement with NRMSE of the testing set, confirming that the F2 model is more capable of predicting responses within the chosen design space. The results in Table VI and graphs in Fig. 2 confirm the defined model for SSA for both formulations. Moreover, NRMSE and comparison between NRMSE of the training and testing sets yielded a better model for F1 formulation, which could not be concluded during the evaluation of the training set. Of particular interest, R^2_{pred} of the model for RT does not correlate with the NRMSE values of the testing set, which further proves the importance of the additional validation experiments and the larger test set. The NRMSE of F1 is even lower for the testing set than for the training set, showing that the right effects and their coefficients are included in the model, which predicts the response well. Regarding the models for RT, the results presented in Tables V and VI show that the models are acceptable for both formulations. The values of NRMSE for the testing and training sets and graphs presented in Fig. 2 show that the model for F1 has a better fit than for F2, which could not be concluded only with data from the training set. A comparison of the model predictions and actual (experimental) values presented in Fig. 2 proves a successful validation of the models. The optimum filling volume of 1 mL and process without annealing were generated, respectively. The model predicted RMC of 0.62 mg (1.26 %, *m*/*m*), SSA 15.58 $m^2\ g^{-1}$, and RT of 4.8 s for F1, whereas experimental values were 0.51 mg (1.04 %, *m*/*m*), 16.3 $m^2\ g^{-1}$, and 2 s, respectively. The model prediction for F2 was 1.256 mg (0.73 %, *m*/*m*) of RMC, 14.991 $m^2\ g^{-1}$ of SSA, and 4.792 s of RT, whereas the experimental values were 1.19 mg (0.69 %, *m*/*m*), 16.8 $m^2\ g^{-1}$, and 5 s, respectively. All three quality attributes match the standard requirements for freeze-dried products; that is, higher SSA, less

than 2 % of RMC, and lower RT. The values are in good agreement and, for these reasons, we strongly believe this approach will yield good predictions. However, we should always bear in mind that models are only approximations to the response, indicating the direction for increasing or decreasing their values.

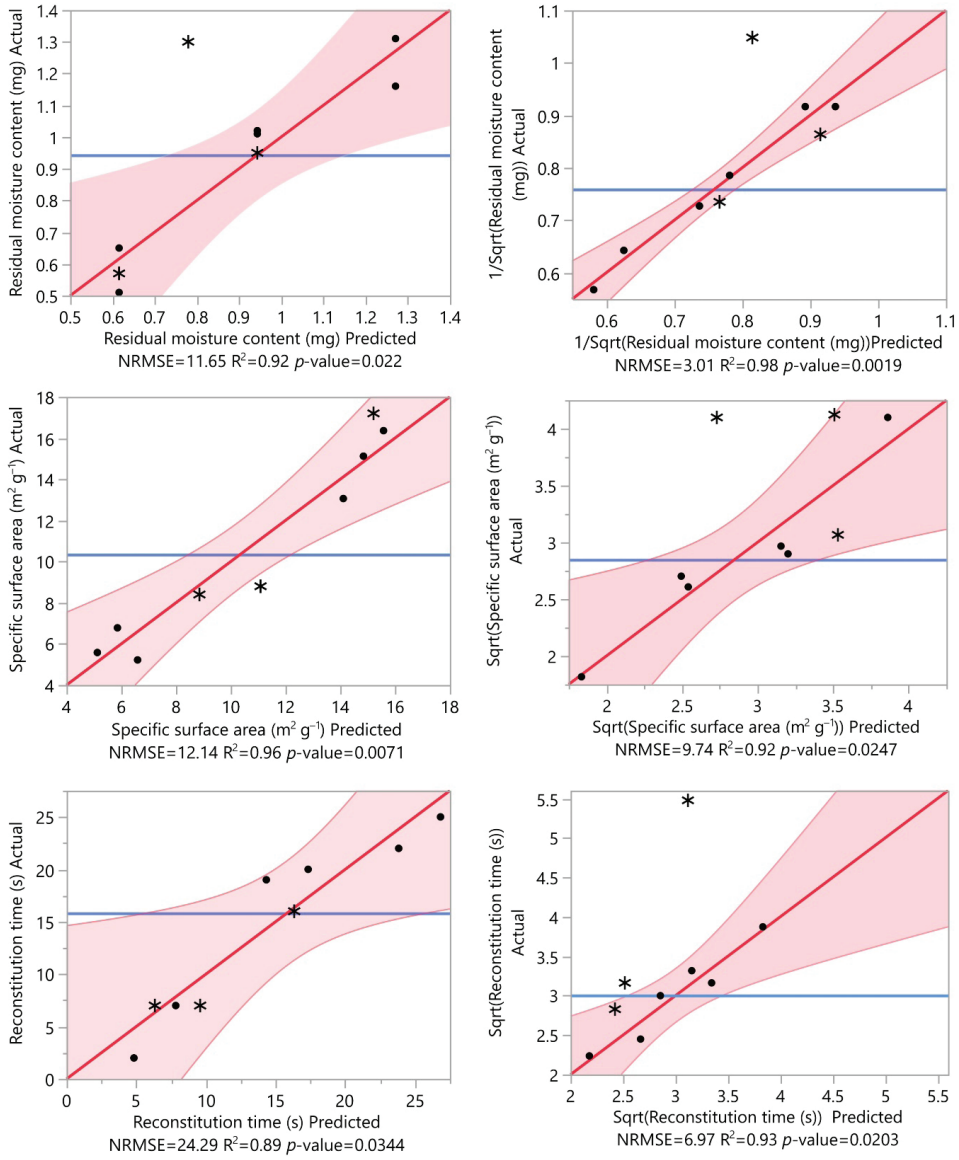

Fig. 2. Actual *vs.* predicted values for F1 (left column) and F2 (right column); (• = training set, ∗ = test set). NRMSE – normalized root-mean-square error, R^2 – coefficient of determination.

CONCLUSIONS

A study of an optimization of the lyophilisation process using a DoE approach with the response surface method was established. The results of this study recommend keeping the filling volume at 1 mL in order to minimize RMC and to avoid the annealing process to maintain a higher SSA of a freeze-dried product. Moreover, the experimental results agreed well with the predictive results and confirmed the high applicability of the tools for future experiments. Such investigation helps in understanding the influence of formulation and process parameters on selected product quality attributes, resulting in an optimized freeze-drying process and a product with constant high quality.

Acknowledgments. – The authors would like to thank the company Krka d.d., Novo mesto for providing support for this study.

Abbreviations. – ANOVA – analysis of variance, BCS – Biopharmaceutical classification system, BET – Brunauer-Emmett-Teller, CM – capacitance manometer, COST – Changing one separate factor at a time, DoE – Design of experiment, DSC – Differential scanning calorimetry, FDM – freeze-dried microscopy, IBP – Ibuprofen, ICH – International Conference on Harmonization, NRMSE – normalized root–mean–square error, NSAID – nonsteroidal anti-inflammatory drug, QbD – Quality by design, PAT – Process analytical technology, R^2 – coefficient of determination, R^2_{adj} – adjusted coefficient of variation, R^2_{pred} – predicted coefficient of determination, RMC – residual moisture content, RMSE – root-mean-square-error, RSM – response surface method, RT – reconstitution time, SSA – specific surface area, T_c – collapse temperature, T_{eu} – eutectic temperature, T_g' – glass transition temperature, T_p – product temperature, T_s – shelf temperature, WFI – water for injection.

REFERENCES

1. A. R. Fernandes, N. R. Ferreira, J. F. Fangueiro, A. C. Santos, F. J. Veiga, C. Cabral, A. M. Silva and E. B. Souto, Ibuprofen nanocrystals developed by 2^2 factorial design experiment: A new approach for poorly water-soluble drugs, *Saudi Pharm. J.* **25** (2017) 1117–1124; https://doi.org/10.1016/j.jsps.2017.07.004
2. J. Nerurkar, J. W. Beach, M. O. Park and H. W. Jun, Solubility of (±)-ibuprofen and S (+)-ibuprofen in the presence of cosolvents and cyclodextrins, *Pharm. Dev. Technol.* **10** (2005) 413–421; https://doi.org/10.1081/PDT-54446
3. K. Stoyanova, Z. Vinarov and S. Tcholakova, Improving ibuprofen solubility by surfactant-facilitated self-assembly into mixed micelles, *J. Drug. Deliv. Sci. Tec.* **36** (2016) 208–215; https://doi.org/10.1016/j.jddst.2016.10.011
4. M. Preskar, T. Vrbanec, F. Vrečer, P. Šket, J. Plavec and M. Gašperlin, Solubilization of ibuprofen for freeze dried parenteral dosage forms, *Acta Pharm.* **69** (2019) 17–32; https://doi.org/10.2478/acph-2019-0009
5. K. T. Savjani, A. Gajjar and J. K. Savjani, Drug solubility: Importance and enhancement techniques, *ISRN Pharm.* **12** (2012) Article ID 195727; http://dx.doi.org/10.5402/2012/195727
6. S. M. Patel and M. J. Pikal, Lyophilization process design space, *J. Pharm. Sci.* **102** (2013) 3883–3887; https://doi.org/10.1002/jps.23703
7. S. Roy, C. Ruitberg and A. Sethuraman, Troubleshooting during the manufacture of lyophilized drug product – Being prepared for the unexpected, *Am. Pharm. Rev.* **15** (2012).
8. T. R. M. De Beer, M. Wiggenhorn, A. Hawe, J. C. Kasper, A. Almeida, T. Quinten, W. Friess, G. Winter, C. Vervaet and J. P. Remon, Optimization of a pharmaceutical freeze-dried product and its process using experimental design approach and innovative process analyzers, *Talanta* **83** (2011) 1623–1633; https://doi.org/10.1016/j.talanta.2010.11.051

9. K. Naelepaa, P. Veski, H. Gjelstrup, J. Rantanen and P. Bertelsen, Building quality into a coating process, *Pharm. Dev. Technol.* **15** (2010) 35–45; https://doi.org/10.3109/10837450902882377
10. International Conference on Harmonisation of Technical Requirements for Registration of Pharmaceuticals and Human use, ICH Harmonised Tripartite Guidelines: Pharmaceutical development Q8 (R2), Current *Step 4* version, August 2009; https://database.ich.org/sites/default/files/Q8_R2_Guideline.pdf; access date, September 20, 2018.
11. V. K. Mourya, Y. Choudhari and M. Padame, Quality by Design: Impact of product variables and their interaction on the particle size in lyophilization of sodium fluoride, *Soft Nanosci. Let.* **6** (2016) 1–10; http://dx.doi.org/10.4236/snl.2016.61001
12. J. Sundaram, Y-H. M. Shay, S. U. Sane and C. C. Hsu, Design space development for lyophilization using Doe and process modelling, *Biopharm. Int.* **23** (2010) 26–36;
13. V. R. Koganti, E. Y. Shalaev, M. R. Berry, T. Osterberg, M. Youssef, D. N. Hiebert, F. A. Kanka, M. Nolan, R. Barrett, G. Scalzo, G. Fitzpatrick, N. Fitzgibbon, S. Luthra and L. Zhang, Investigation of design space for freeze-drying: Use of modeling for primary drying segment of a freeze-drying cycle, *AAPS PharmSciTech*. **12** (2011) 854–861; https://doi.org/10.1208/s12249-011-9645-7
14. A. G. Martinez, B. E. Rodrigez, A. P. Roca and A. M. Ruiz, Intravenous ibuprofen for treatment of post-operative pain: A multicenter, double blind, placebo-controlled, randomized clinical trial, *PloS One* **11** (2016) 1–16; https://doi.org/10.1371/journal.pone.0154004
15. D. Awotwe-Otto, C. Agarabi and M. A. Khan, An integrated process analytical technology (PAT) approach to monitoring the effect of supercooling on lyophilization product and process parameters of model monoclonal antibody formulations, *J. Pharm. Sci.* **103** (2014) 2042–2052; https://doi.org/10.1002/jps.24005
16. S. M. Patel, S. L. Nail, M. J. Pikal, R. Geidobler, G. Winter, A. Hawe, J. Davagnino and S. R. Gupta, Lyophilized drug product cake appearance: What is acceptable, *J. Pharm. Sci.* **106** (2017) 1706–1721; http://dx.doi.org/10.1016/j.xphs.2017.03.014
17. J. C. Kasper and W. Friess, The freezing step in lyophilisation: Physico-chemical fundamentals, freezing methods and consequences on process performance and quality attributes of biopharmaceuticals, *Eur. J. Pharmaceut. Biopharmaceut.* **78** (2011) 248–263; http://doi.org/10.1016/j.ejpb.2011.03.010
18. E. Meister, A significant comparison between collapse and glass transition temperatures, *Eur. Pharm. Rev.* **13** (2008) 73–79.
19. J. Horn and W. Friess, Detection of collapse and crystallization of saccharide, protein and mannitol formulations by optical fibers in lyophilization, *Front. Chem.* **6** (2018) 1–9; https://doi.org/10.3389/fchem.2018.00004
20. G. Assegehegn, E. B.- de la Fuente, J. M. Franco and C. Gallegos, The importance of understanding the freezing step and its impact on freeze-drying process performance, *J. Pharm. Sci.* **108** (2019) 1378–1395; https://doi.org/10.1016/j.xphs.2018.11.039
21. S. M. Patel, C. Bhugra and M. J. Pikal, Reduced Pressure Ice Fog technique for controlled ice nucleation during freeze-drying, *AAPS PharmSciTech* **10** (2009) 1406–1411; https://doi.org/10.1208/s12249-009-9338-7
22. W. Abdelwahed, G. Degober and H. Fessi, Freeze-drying of nanocapsules: Impact of annealing on the drying process, *Int. J. Pharm.* **324** (2006) 74–82; https://doi.org/10.016/j.ijpharm.2006.06.047
23. M. S. Arshad, Application of through-vial impedance spectroscopy as a novel process analytical technology for freeze drying, Phd Thesis, Leicester School of Pharmacy, De Montfort University, 2014; https://www.dora.dmu.ac.uk/xmlui/bitstream/handle/2086/10407/PhD%20Thesis%20Sohail%20Muhammad%20Arshad%20After%20corrections%20KW_JB_WS_GS%20approved.pdf;sequence=1, access date August 2, 2018.
24. G. Smith, M. S. Arshad, E. Polygalov and I. Ermolina, Through-vial impedance spectroscopy of the mechanisms of annealing in the freeze-drying of maltodextrin: The impact of annealing hold

time and temperature on the primary drying rate, *J. Pharm. Sci.* **103** (2014) 1799–1810; https://doi.org/10.1002/jps.23982

25. P. Fonte, S. Reis and B. Sarmento, Facts and evidences on the lyophilisation of polymeric nanoparticles for drug delivery, *J. Control. Release* **225** (2016) 75–86; https://doi.org/10.1016/j.jconrel.2016.01.034
26. X. Tang and M. J. Pikal, Design of freeze-drying processes for pharmaceuticals: practical advice, *Pharm. Res.* **21** (2004) 191–200; https://doi.org/10.1023/b:pham.0000016234.73023.75
27. X. Lu and M. J. Pikal, Freeze-drying of mannitol-trehalose-sodium chloride-based formulations: The impact of annealing on dry layer resistance to mass transfer and cake structure, *Pharm. Dev. Technol.* **9** (2004) 85–95; https://doi.org/10.1081/PDT-120027421
28. L. Rey and J. C. May, *Freeze Drying/Lyophilization of Pharmaceutical and Biological Products*, 3rd ed., Informa Healthcare, New York, London 2011.
29. G. Smith, E. Polygalov, M. S. Arshad, T. Page, J. Taylor and I. Ermolina, An impedance-based process analytical technology for monitoring the lyophilisation process, *Int. J. Pharm.* **449** (2013) 72–83; http://dx.doi.org/10.1016/j.ijpharm,2013.03.060
30. J. Frost, *Multiple Regression Analysis: Use Adjusted R-Squared and Predicted R-Squared to Include the Correct Number of Variables*; https://statisticsbyjim.com/regression/interpret-adjusted-r-squared-predicted-r-squared-regression/; access date November 11, 2019
31. A. Hayes, *R-Squared Definition*, Updated May 8, 2019 https://www.investopedia.com/terms/r/r-squared.asp; access date November 11, 2019
32. S. Raissi and R.-E. Farsani, Statistical process optimization through multi-response surface methodology, *Int. J. Math.Comput. Sci.* **3** (2009) 197–201.
33. D. Bas and I. H. Boyaci, Modelling and optimization I: Usability of response surface methodology, *J. Food Eng.* **78** (2007) 836–845; https://doi.org/10.1016/j.jfoodeng.2005.11.024